SUPPLEMENTARY INFORMATION for:

Distorted Insights from Human Mobility Data

Riccardo Gallotti,[1, a)] Davide Maniscalco,[1] Marc Barthelemy,[2, 3] and Manlio De Domenico[4, 5, 1, b)]

[1)] *Fondazione Bruno Kessler, Via Sommarive 18 38123 Povo (TN), Italy*

[2)] *Université Paris-Saclay, CNRS, CEA, Institut de Physique Théorique, 91191, Gif-sur-Yvette, France*

[3)] *CAMS (CNRS/EHESS) 190-198, avenue de France, 75244 Paris Cedex 13, France*

[4)] *CoMuNe Lab, Department of Physics and Astronomy "Galileo Galilei", University of Padua, Italy*

[5)] *Istituto Nazionale di Fisica Nucleare, Sez. Padova, Italy*

[a)] Electronic mail: rgallotti@fbk.eu

[b)] Electronic mail: manlio.dedomenico@unipd.it

SUPPLEMENTARY NOTE: TECHNICAL LIMITATIONS AFFECTING HUMAN MOBILITY DATASETS

In this manuscript, we observe great differences in how mobility datasets coming from different providers are able to describe mobility flows at a country level. In this section of the Supplementary Materials, we briefly discuss here a series of possible causes for the differences. This list does not however represent a comprehensive text illustrating all biases associated with mobility data collection and elaboration, for which we suggest further readings[4–8].

Behaviour captured

Most datasets discussed are being passively collected from ICT data records. They are therefore necessarily influenced by the type of behaviour that produces the records. Issues associated with the behaviour captured cannot in general be solved, but awareness of the consequences of passive collection of movement behaviour can limit the errors introduces in the analysis.

Mobile Phone Call Detail records used to be associated with phone calls and SMS messages. Consequently, displacements between CDR records only represents movements between phone communications[9]. But as the use of the "mobile data" connection has become widespread, the datasets captured are now less coupled with the communication behaviour, but can still be limited by the closure of the data connection by users.

Providers aggregating data from several mobile apps, such as Cuebiq or Safegraph, and on a broader sense also Google and Facebook, capture data when the device GPS connection is used by one of the location based applications associated with the providers, which may require the user to be actively using that app or not, depending on the specifics of the app.

Other GPS data such those of Octotelematics coming from devices installed to cars for insurance reason, but also data from Tomtom data coming from single apps specifically gathering the movements of bikers or runners, are necessarily limited to movements associated with a specific mode of transport.

Finally, the accuracy of census data can be hindered by the tendency of users to not update their records in case of relocation. This tendency may depend upon the incentives set by each country for this update (for example, in the case of Italy, citizens are highly incentivised to update their public records to have access to the Public Health System).

Segmentation and sampling

Mobility data is generally gathered in form of raw trajectories formed by a sequence of position where a user has been observed at a certain time. For understanding the user movement behaviour, these trajectories are usually segmented into a sequence of movements in space and stops where the user stays in a particular place for a certain duration in time. There are several alternative methods for this segmentation. Many data provider designed their own optimised for their data which details are often undisclosed private. The observed segmented results can be very sensitive to algorithmic and parametric choices, as discussed in[10,11]. The impact of this issue can be reduced for academic use by allowing to operate directly on the raw trajectories using open source methods with explicit parametric choice.

Spatial Granularity

Segmented trajectories are, in most cases, further aggregated over (administrative) areal units to obtain the so-called Origin-Destination (OD) matrices. The choice of those areal units clearly influences the observed results, a problem known in literature as "Modifiable areal unit problem". Many datasets circulating are influenced by this problem. In Supplementary Figure 12, we illustrate this with an example using it on our main indicator, the displacement distribution $P(L)$. In panel (a) we show how the distances estimated between the centroids of the unit areas may differ from the average distance of users moving between these areas, while in panel (b) we show how different spatial granularity yields to different observed $P(L)$. While this problem is intrinsic with the choice of aggregating data for obtaining a flow matrix, allowing researchers to use the granularity most adapt to the analysis performed instead to adapting to a standard one chosen by the data provider can without any doubt limit the biases introduced.

Upscaling

All data gathered, with the exception of Census, describe only a fraction of the total population. Often, for ICT-based datasets, the representativity of this sample is also biased towards high-income, more urban and mostly male populations. To estimate the real mobility flows of the whole population between different areas, that is the information captured in the OD matrices, it is necessary to "upscale" the observed flows. Several methods can be used for upscaling, in most case they are based on a proportionality with respect to an estimate of the local observed population. The knowledge of the active populations in each areal unit, which could also be a function of time, becomes therefore a crucial piece of information to rebalance the observed flows to what is expected to be the mobility of the total population. Lack of knowledge about active population can conversely limit the analysis due to the need of having more imprecise upscaling. This issue can be easily solved by the company, by providing explicit information about the user-base population as a function of time (as Facebook and Cuebiq do in the data analysed in this paper), when possible with data disaggregated by income and gender in order to allow for alleviating the potential biases in the data using post-stratification methods.

Self-loops

For many applications, knowing how large is the fraction of people who exited an areal unit with respect to those who circulated only locally is very relevant. This information is captured, in an OD matrix, in the diagonal elements that describe, from a network perspective, self-loops of the mobility flows network. This self loops are in general present in most aggregated datasets. However, it is often not very clear what they do represent. It can encompass at the same time information on the number users observed in the dataset, i.e. those activate the capturing device but never left their home location. Or alternatively users who performed a local movement (as identified by the segmentation algorithm), but never arriving at leaving the areal unit. Unless specified, it is in principle not clear if users who belong to the self loop are also counted it outwards flows. All this info information can be very relevant for mobility analysis and epidemic modelling and we advise, as a minimum, to describe clearly what is represented by self loops and to further include any other "non movement" information available among the information accompanying the OD matrices.

Pruning

In all datasets, small flows between two areas can be unobserved because of the local user-base population is too small or because the behaviour captured or the segmentation method has a limited efficiency at identify the users' movement. This makes the observed OD matrices systematically sparser than the real ones. This effect is further worsened by an active "pruning" of the mobility network done to limit the size of the datasets shared and to ensure K-Anonymity. As discussed in the paper, in the Facebook data we estimated that the pruning happens for flows below (10 users)/(8 hours), while Google declare cuts below 100 users/week, and this pruning heavily influences our possibility of using the data collected for studying long-range mobility. This major problem can be solved, again, by providing to researcher a way of elaborating directly raw data without applying any heavily lossy pre-elaboration such as pruning.

Fragmentation

Again for limiting the size of data archives, the datasets provided are often divided into large administrative ares (countries, US states, ...). Similarly to pruning, also this process forcefully cuts long range mobility. This problem can be illustrated by the data provided by Facebook for USA, where they used state-level fragmentation, not allowing for any analysis about the spreading behaviour across the continental USA. Spreading processes over wide areas is more than the sum of the spreading processes over its parts. The issue of fragmentation is unfortunately not easy to solve, as in many cases the data providers only has data associated to a single country. This makes the problem of studying international flow one of the hardest we face. Only a few sources have international coverage, but aviation data are limited to a single mode of transport that can underestimate mobility between contiguous countries. Google data, as we saw, is heavily influenced by pruning cutting long range flows and Facebook offers only fragmented data. We believe that this great limitation in the opportunity of analysing international flows, information nowadays so vital for epidemic containment, represent a paradigmatically example illustrating the need of a shared platform where to share, elaborate and analyse mobility data for academic purposes.

SUPPLEMENTARY FIGURES

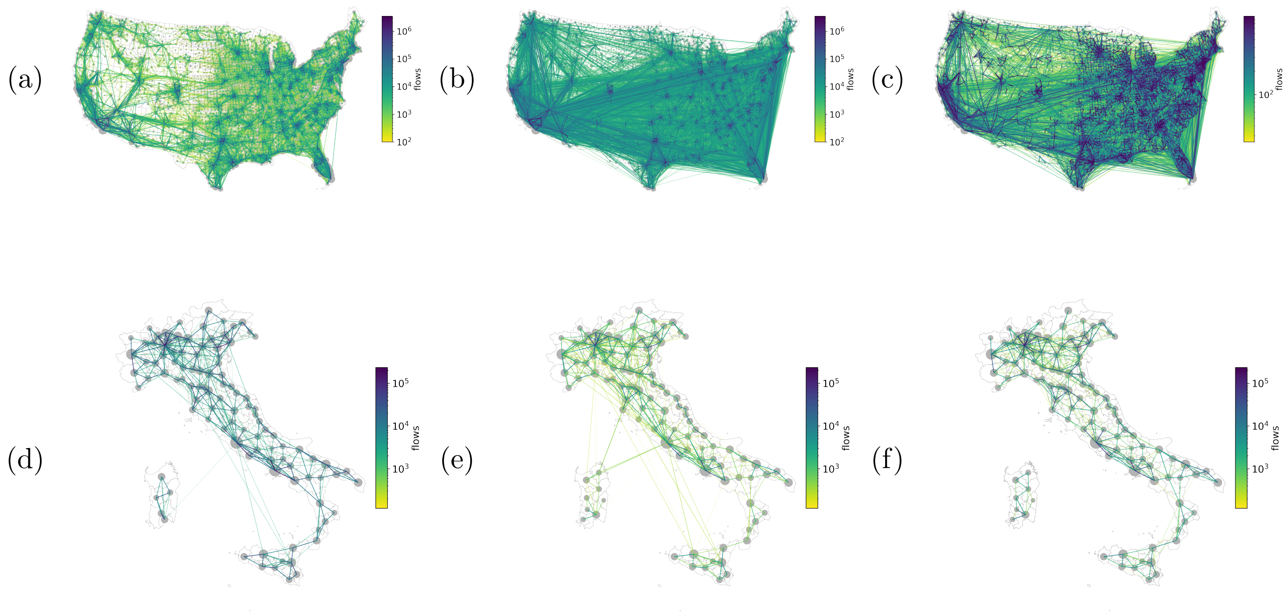

Supplementary Fig. 1. **Visual comparison of baseline flow maps selecting a fixed number of high flow edges.** Here we display the same networks displayed in Fig.1, but limiting each network to having at max the number of edges of the sparser network of the same country by removing edges with smaller flows. For U.S.A. we have Cuebiq **(a)** which is the sparser, Safegraph **(b)** and Census **(c)**. Here networks are visibly different even if one compensate for the different edge density. For Italy we have Cuebiq **(d)**, Facebook **(e)** and Census **(f)**. In this case, the differences between networks are less pronounced, with as the only observable difference the lack of connectivity between the peninsula and the islands of Sardigna and Sicily for Census data (panel c)

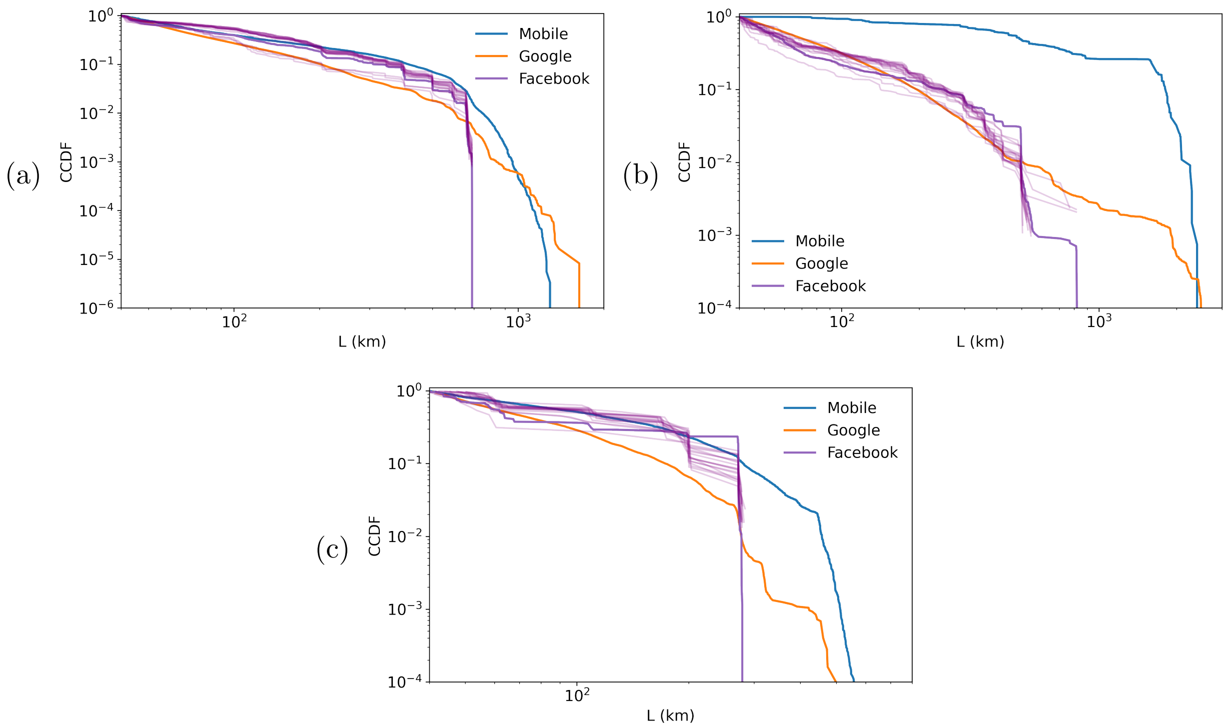

Supplementary Fig. 2. **The Displacement Distributions of France (a), Spain (b), Portugal (c).** Here, we rescaled the mobile data coming from[12] to become representative of the underlying population similarly to what done with Cuebiq and Facebook data. The light purple lines represent the evolution in time of the Facebook dataset, while the thick line represents the baseline. The differences associated with the COVID-19 lockdown, one of the more impactful events in world history, is smaller than the observed difference between datasets.

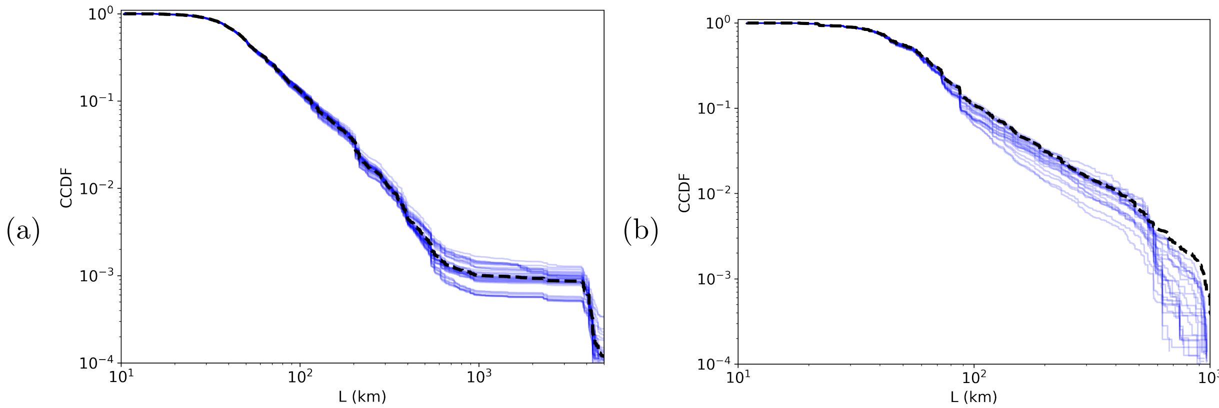

Supplementary Fig. 3. **The evolution in time of the Cuebiq data in the USA (a) and Italy (b)** Again, the differences associated with the COVID-19 lockdown is smaller than the observed difference between datasets. There the CCDF is analyzed for $L > 10$ and not limited to the continental U.S.A. The black dashed line represents the baseline curve.

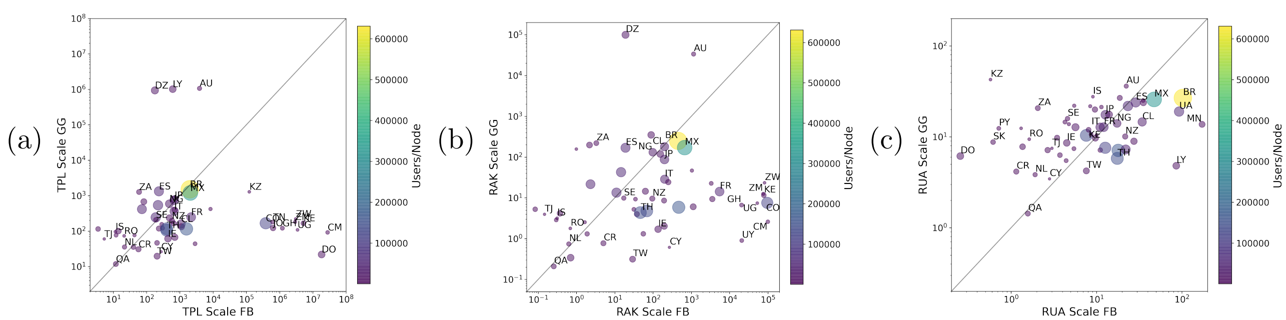

Supplementary Fig. 4. **Comparison of the scale parameters fitted for Facebook and Google datas with different models.** We illustrate here the difference between the fitted parameters for a set of 58 countries that are present in both the Facebook and the Google datasets. In panels a) and b) we represent the scale parameter of two bi-dimensional fits (truncated power law $P(L) \propto L^{-\alpha} e^{\frac{L}{L_s}}$ and the saddle point approximation of the random acceleration kicks model $P(L) \propto L^{-\alpha} e^{\left(\frac{L}{L_s}\right)^{0.5}}$). Due to the very sensible degree of freedom associated with the scaling parameter, the differences observed in the distance scale L_s are way larger than what observed in c), where the scale is estimated using the monoparametric random uncorrelated acceleration model ($P(L) \propto L^{-0.75} e^{\left(\frac{L}{L_s}\right)^{0.5}}$)

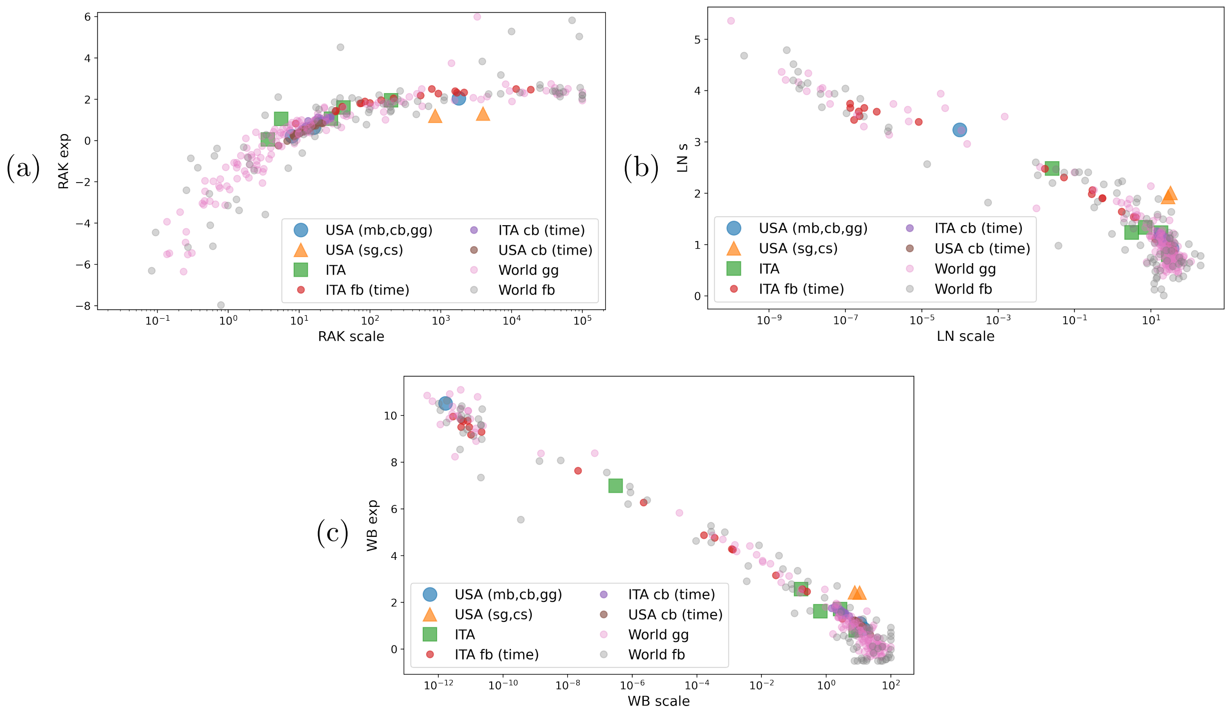

Supplementary Fig. 5. **Comparison of the displacement distributions across the globe.** We observe a wide variance in the fit parameters estimated for the $P(L)$. In panels (a), (b), and (c) we represent the the scale and exponent parameter for the Random Acceleration Kicks models, a Lognormal fit, and a Weibull fit respectively. As in Fig. 2, we include the curves of Fig. 1 for USA – Cuebiq (cb), Mobile (mb)^2, Google (gg), Safegraph (sg), Census (cs) – and Italy (that, as illustrated in Fig. 1 includes also Octotelematics and Facebook (fb) data). The multiple values for the longitudinal weekly analysis of Cuebiq and Facebook data, and the values estimated for the Google and Facebook baseline worldwide, are indicated as smaller circles. We observe how all data points align around a curve, which suggests strong correlation between the free parameter and, ultimately, the existence of an underlying law having a single degree of freedom.

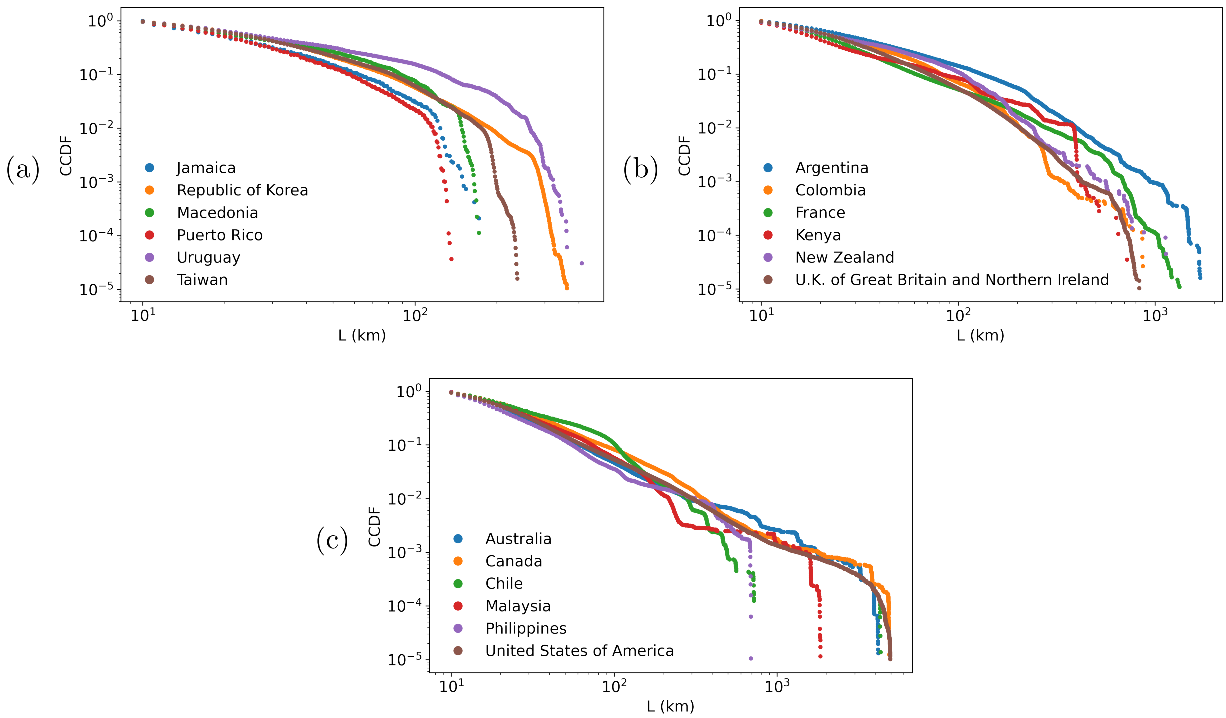

Supplementary Fig. 6. **Comparison of the displacement distributions across the globe.** Using the Google dataset, we observe how the tail behaviour of $P(L)$ is radically different if one consider small or insular countries (a), medium size countries (b),or large countries or archipelagos (c). These subsets of countries have been identified using the RAK fits as large countries have an exponent > 2, the medium size countries have been selected between those with exponent between 0 and 1 and the small countries have exponent < -3. In the smaller countries we observe an exponential-like cutoff, while in the larger countries the curves are more stretched and suggest the existence of multiple scales.

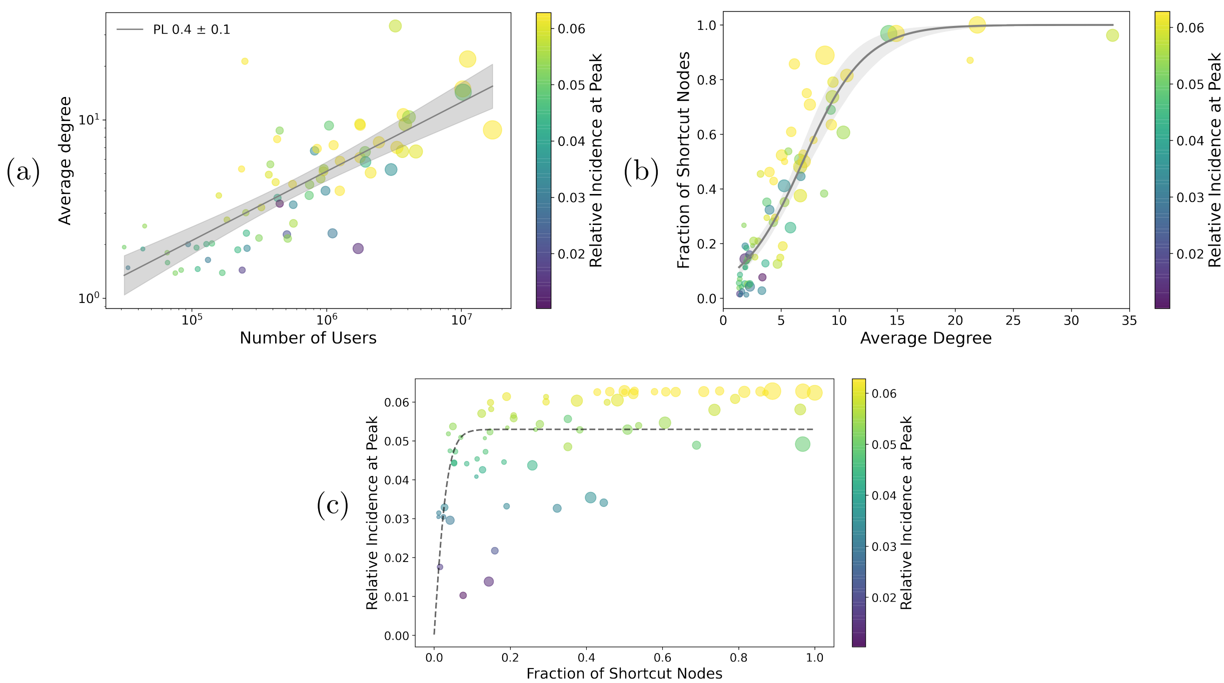

Supplementary Fig. 7. **Small world effect in epidemic diffusion.** (a) Focusing on a single dataset, the Facebook baseline mobility, we observe how the average number of edges per node grows as the number of users increases (the fit suggest a scaling sub-linear behaviour). This is most likely due to a pruning procedure that removes edges with smaller flows for both privacy enhancing and disk space reduction. However, introducing a threshold to minimal flow (we estimate is about 10 users/8 hours for these data) systematically cuts longer edges where movement costs are higher, and in particular between marginal areas. (b) This reflects into a great change into the shape of the network. Networks with higher average degree has a larger fraction of shortcut nodes (where shortcuts are defined as links at least 2 times as long as the average distance between a node and the closest neighbour). The fit here suggests a logistic behaviour. (c) The fraction of shortcut nodes, in turn, determines the behaviour of spreading processes on the network, here again we illustrate it over the Facebook baseline mobility networks. As we did also in Fig. 3 and Supplementary Fig. 11, we simulate the spreading of epidemics using a SIR model starting from a single seed in the node with the larger userbase. We see how when the fraction of shortcut nodes passes a relatively small threshold, we have consistently a faster spreading and thus a higher incidence at peak.

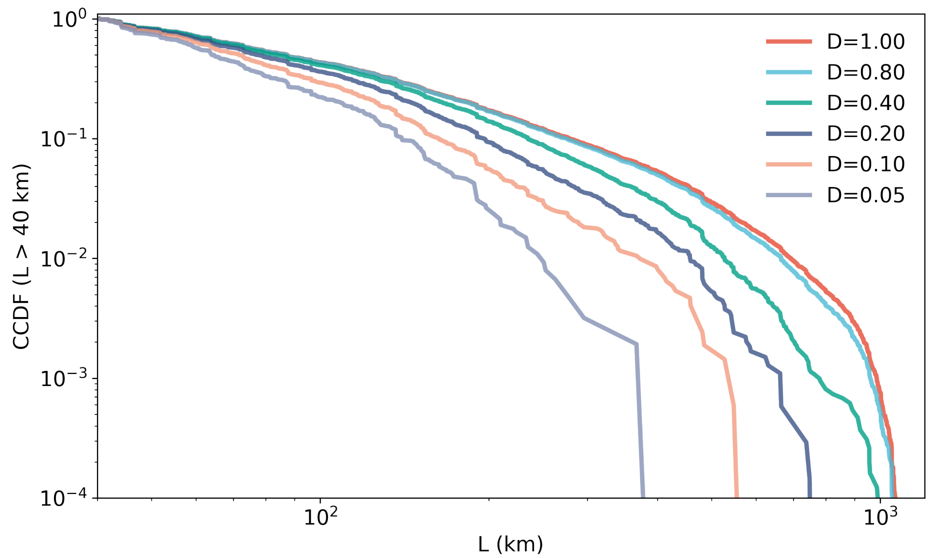

Supplementary Fig. 8. **Displacement distribution of a pruned gravity-generated network.** Starting with resident population of Italy at province level, we generated the flow with a toy Gravity model as $\phi_{i,j} \propto P_i P_j L_{i,j}^{-2}$ where P_i is the population at node i and $L_{i,j}$ the distance between nodes i and j. Then, we progressively removed edges having the smallest flows until reaching an edge density D indicated in the figure legend. This process strongly influences the observed $P(L)$ when $D < 0.8$. Now, as seen in Table I empirical edge densities are lower than 0.35 in all three Italian datasets, suggesting that a significant part of long flows might be missing in the data captured.

(a)

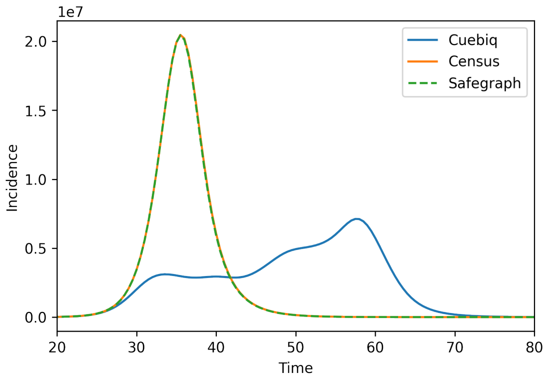

(b)

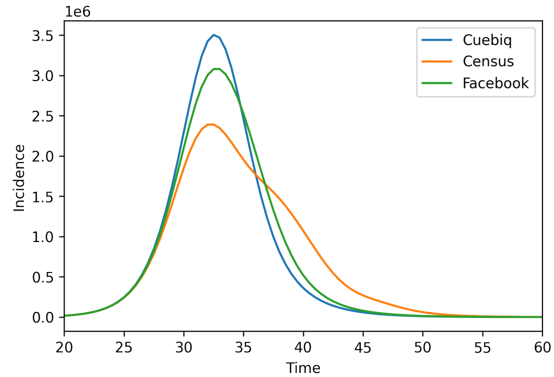

Supplementary Fig. 9. **Effect of different datasets on spreading dynamics.** Here we represent the differences between the spreading dynamics in U.S.A. and Italy using the SIR model described in the paper. We present the evolution over time of the incidence, that accounts for the new infected in that unit time. In panel (a), we see how for U.S.A. Safegraph and Census (solid orange and dashed green lines), that as we discussed are characterized by an significantly larger weight of long range flows, yield exactly the same result that likely is equivalent to homogeneous mixing. Since Cuebiq data does not display this over-abundance of long range connections, the epidemic diffusion is mostly local (see Supplementary Fig. 10) and produces a more complex behaviour where the incidence curve has two peaks. In panel (b), Italian data display instead smaller differences, probably because of the smaller spatial scale of the Italian peninsula with respect to the spatial scales at hand. Here the peak appear not delayed but rather lowered for Facebook and Census data, that are in this case characterized by an under-representation of long-range connections.

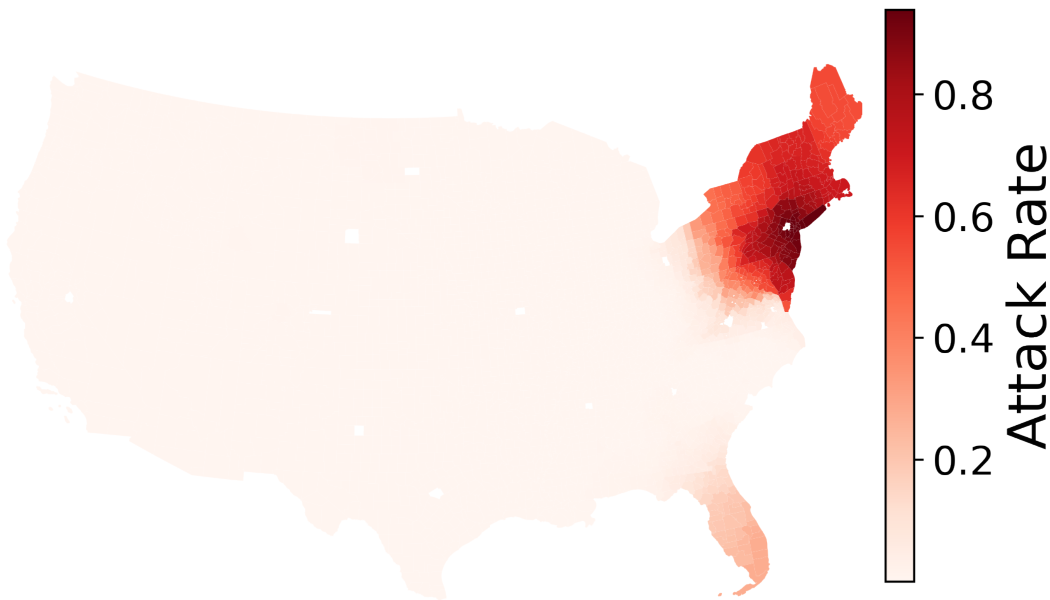

Supplementary Fig. 10. **Mapping of the attack rate across U.S.A. at the first epidemic peak simulated with Cuebiq data.** The map represents the epidemic state in correspondence of the first peak in the U.S.A. Cuebiq simulation (day 40). The epidemics, starting in Manhattan (NY), appear geographically contained and spreading only locally. On the other hand, the equivalent Safegraph and Census plot would show a map of the U.S.A. homogeneously red.

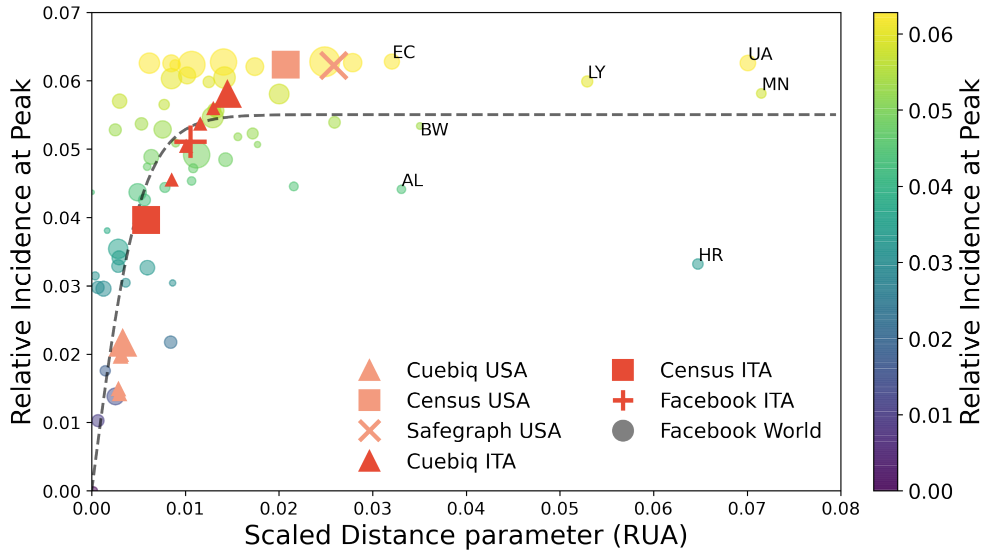

Supplementary Fig. 11. **Understanding the small world effect in epidemic diffusion by fitting the $P(L)$** The relative incidence at peak, that is the largest fraction of population that become infected in a single day during the epidemic simulation, can be reconnected to the property of the $P(L)$. We use here the scale parameter of the $P(L)$ estimated using the RUA model, that being characterized by a single parameters yields the more stable estimate for the spatial scale (see Supplementary Fig. 4). This relative scale parameter is, for each country, obtained by dividing the RUA scale parameter by the maximal length of the continental landmass, estimated as the longest side of a minimum rotated rectangle shape of the continental outline of the country). We analyse in this plot not only the Facebook baseline, but also the networks illustrated in Figure 1 and observe clearly how to larger relative values of the relative RUA scale, that we can associated to a larger tendency to small world behavior and, similarly to what observed in Supplementary Fig. 7 (c), we have that larger scale mobility dictates significantly larger epidemic effects. At the same time, as observed in Fig. 3, we also observe great variation in the incidence at peak in the same country depending on the different source of data used.

(a) 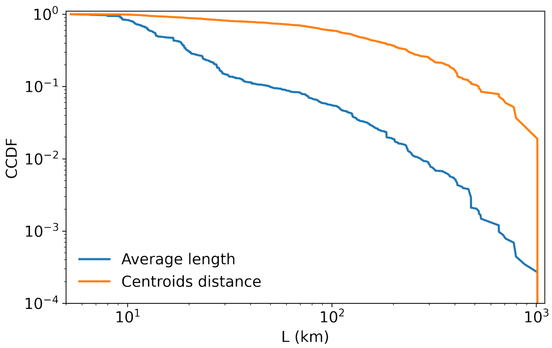

(b) 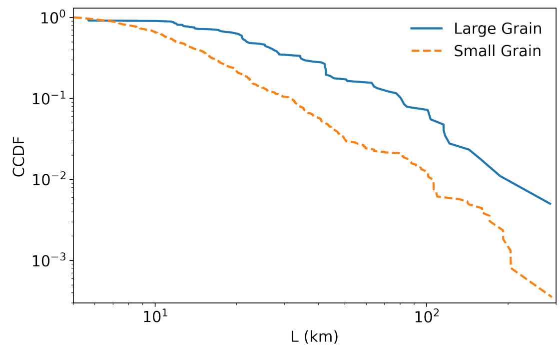

Supplementary Fig. 12. **Analysis of the effects of granularity on Facebook baseline data.** **a)** the differences in the $P(L)$ distribution function in Italy changes if one consider as displacement lengths the distance between the centroids of the administrative areas or the average length indicated by Facebook. From this graph, we can deduce that the real displacements are remakably smaller than what estimated using the centroid distance. **b)** the differences in the $P(L)$ distribution function in Hungary changes if one consider two different areal units lengths. The Hungarian datasets comes replicated with two different granularities, one consistent with the other countries (here indicated as Large grain), having 20 nodes, another with a smaller areal unit, having 821 nodes. We observe a wide difference between the displacement distribution estimated using the average lengths over these two datasets, with the larger grain dataset yielding larger distances estimates over the same dataset.

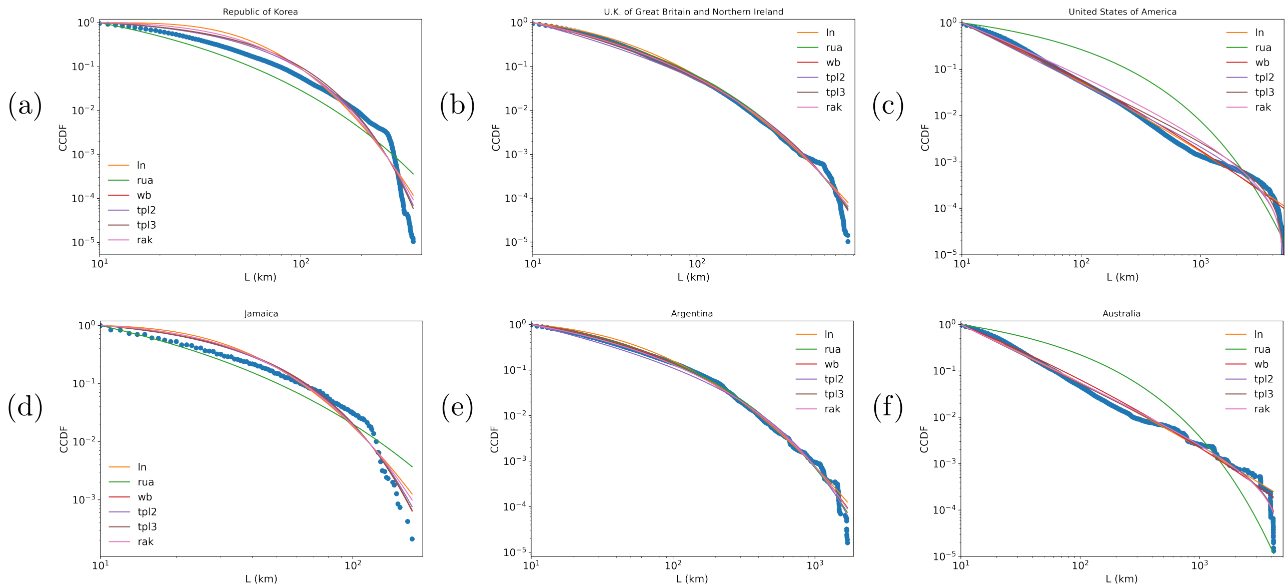

Supplementary Fig. 13. **Comparison of the best-fits of the displacement distribution for countries of different sizes.** We illustrate here the alternative fits executed on Google data using the models described in the Methods. We can appreciate how the fits appear to be well converged. For mid-size countries (UK and Argentina), the alternative fit functions give very similar results. For smaller (Republic of Korea, Jamaica) or larger (U.S.A. or Austraila) countries, the observed behavior diverges from what it can be fit with the models proposed, especially for the monoparametric RUA model.

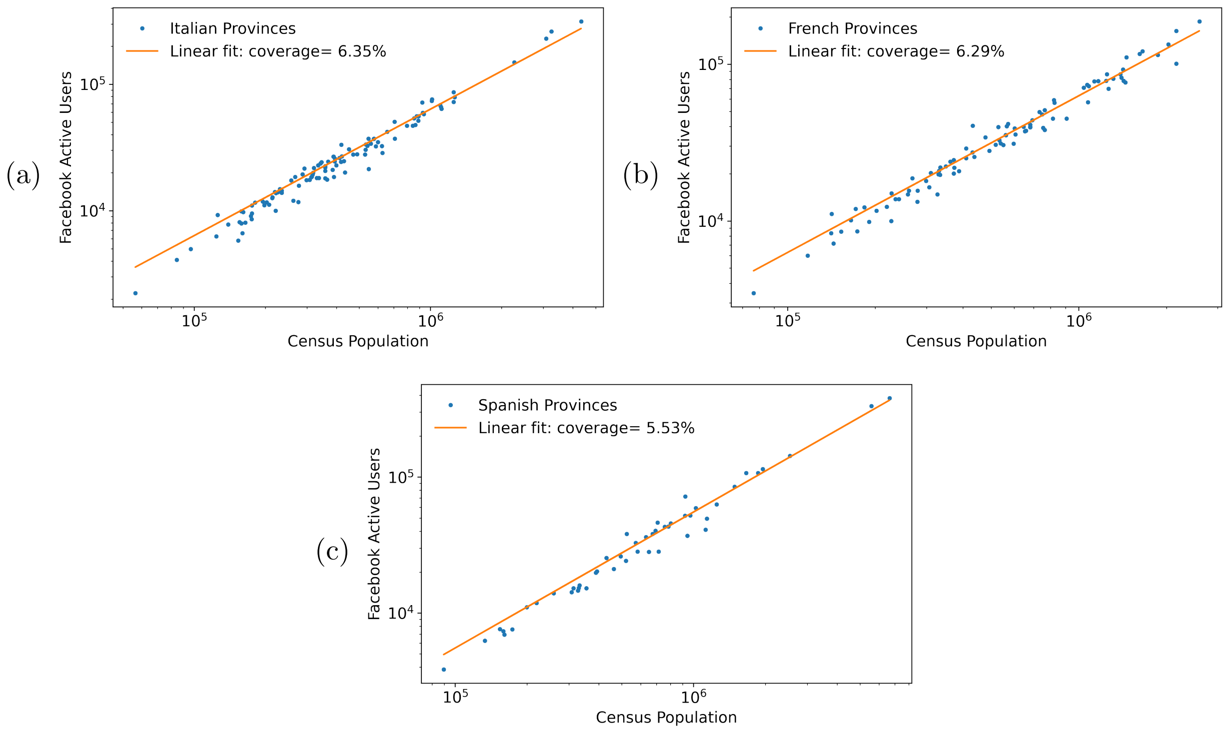

Supplementary Fig. 14. **Comparison between Census population and Facebook Active Users at province level in Italy (a), France (b) and Spain (c)** In all three European countries, the fraction of population covered by the Facebook dataset is larger than 5% and Spearman correlations are strong and highly significant (Italy $r = 0.980$, $p \approx 10^{-78}$), (France $r = 0.984$, $p \approx 10^{-71}$), (Spain $r = 0.978$, $p \approx 10^{-33}$). These numbers strongly support the use of the Facebook active user base as a proxy for the resident population.

SUPPLEMENTARY TABLES

Provider	Source	Area	Elaboration	Precision	Stop time	NW Aggregation	Self-loops	Pruning	Availability
Teléfonica[13]	Mobile Phone	Germany	Authors	Cell tower	15 min	NUTS3 / weekly	Yes	$\phi < 5$	Restricted
Facebook[14,15]	Social Media Access	Several countries	Company	GPS	?	Administrative / 8 hours	Yes	Yes	Data4good
Orange[16]	Mobile Phone	France	Authors	Cell tower	1 hour	Municipality / weekly	Yes	?	Restricted
Baidu[17,18]	Location Based Service	China	Company	?	?	Province / daily	Yes	?	Restricted
Baidu[19]	Location Based Service	China	Company	?	?	Prefecture / daily	Yes	?	Restricted
Cuebiq HDR[20]	Mobile Apps	Italy	Authors	GPS	5 min	Province / daily	Yes	No	Public
Teléfonica[21]	Mobile Phone	Colombia	Authors	Cell tower	day	Department / daily	Yes	No	Restricted
Google[19]	Location History	Worldwide	Company	5km^2 area	?	Municipality / weekly	(Yes)	Yes	Restricted
Google[19]	Location History	Italy	Company	5km^2 area	?	Province / weekly	(Yes)	Yes	Restricted
Google[22]	Location History	Europe	Company	(5km^2 area)	?	Country / beweekly	(Yes)	Yes	Restricted
Google[23–25]	Location History	Intra-Urban	Company	(5km^2 area)	?	Weekly	Yes	Yes	Restricted
Safegraph[26]	Mobile Apps	USA Metro areas	Authors	PoI	?	Census Block/Weekly	?	Yes	Data4Good
Safegraph[27]	Mobile Apps	USA	Authors	PoI	?	Census Block/Daily	Yes	Yes	Public

Supplementary Table I. **Characteristics of the datasets used for modeling the epidemic spreding of COVID-19.** Note: the Google dataset is in principle also part of a Data4good initiative and accessible upon request, however we started the request procedure more than a year and a half ago and our demand is still "under consideration". Information between parenthesis has been found in a different paper on the same dataset.

Dataset Name	Information Available	Area(s) of Analysis	Period of Analysis	Reference
Census ITA	OD Flows	Italy	2011	istat.it[28]
Census USA	OD Flows	U.S.A	2015	census.gov[29]
Cuebiq ITA	OD Flows	Italy	January-June 2020	Pepe et al. (2020)[20]
Cuebiq USA	OD Flows	U.S.A	January-September 2020	Cuebiq Data for Good program[30]
Facebook	OD Flows	Worldwide	(2020-2021)	Facebook Data for Good program[31]
Gonzalez 2008	$P(L)$ PDF (fit parameters)	U.S.A.	?	Gonzalez et al. (2008)[2]
Google	$P(L)$ PDFs	Worldwide	2016	Kraemer et al. (2020)[1]
Mobile FRA	OD Flows	France	2007	Tizzoni et al. (2014)[12]
Mobile ESP	OD Flows	Spain	2007	Tizzoni et al. (2014)[12]
Mobile POR	OD Flows	Portugal	2006	Tizzoni et al. (2014)[12]
Octotelematics	$P(L)$ PDF	Italy	May 2011	Gallotti et al. (2016)[3]
Safegraph	OD Flows	U.S.A	2019-2021	Kang et al. (2020)[27]

Supplementary Table II. **List of data sources used in this paper.** In this work, we integrated data from numerous sources and available in different formats. From Origin-Destination Flow data (OD Flows) we derived the Probability Distribution Functions (PDF) for the displacement distributions to compare with those. The period of analysis of Facebook data varied depending on the single country data.

SUPPLEMENTARY REFERENCES

[1]Kraemer, M. U. G. *et al.* Mapping global variation in human mobility. *Nature Human Behaviour* **4**, 800–810 (2020).

[2]Gonzalez, M. C., Hidalgo, C. A. & Barabasi, A.-L. Understanding individual human mobility patterns. *Nature* **453**, 779–782 (2008).

[3]Gallotti, R., Bazzani, A., Rambaldi, S. & Barthelemy, M. A stochastic model of randomly accelerated walkers for human mobility. *Nature communications* **7**, 1–7 (2016).

[4]Ranjan, G., Zang, H., Zhang, Z.-L. & Bolot, J. Are call detail records biased for sampling human mobility? *ACM SIGMOBILE Mobile Computing and Communications Review* **16**, 33–44 (2012).

[5]Bonnel, P., Hombourger, E., Olteanu-Raimond, A.-M. & Smoreda, Z. Passive mobile phone dataset to construct origin-destination matrix: potentials and limitations. *Transportation Research Procedia* **11**, 381–398 (2015).

[6]Olteanu, A., Castillo, C., Diaz, F. & Kıcıman, E. Social data: Biases, methodological pitfalls, and ethical boundaries. *Frontiers in Big Data* **2**, 13 (2019).

[7]ESCAP, U. Handbook on the use of mobile phone data for official statistics (2019).

[8]De Broe, S. *et al.* Updating the paradigm of official statistics: New quality criteria for integrating new data and methods in official statistics. *Statistical Journal of the IAOS* **37**, 343–360 (2021).

[9]Zhao, Z. *et al.* Understanding the bias of call detail records in human mobility research. *International Journal of Geographical Information Science* **30**, 1738–1762 (2016).

[10]Gallotti, R., Louf, R., Luck, J.-M. & Barthelemy, M. Tracking random walks. *Journal of The Royal Society Interface* **15**, 20170776 (2018).

[11]Zhao, P., Haitao, H., Li, A. & Mansourian, A. Impact of data processing on deriving micro-mobility patterns from vehicle availability data. *Transportation Research Part D: Transport and Environment* **97**, 102913 (2021).

[12]Tizzoni, M. *et al.* On the use of human mobility proxies for modeling epidemics. *PLoS computational biology* **10**, e1003716 (2014).

[13]Schlosser, F. *et al.* Covid-19 lockdown induces disease-mitigating structural changes in mobility networks. *Proceedings of the National Academy of Sciences* **117**, 32883–32890 (2020).

[14] Bonaccorsi, G. *et al.* Economic and social consequences of human mobility restrictions under covid-19. *Proceedings of the National Academy of Sciences* **117**, 15530–15535 (2020).

[15] Galeazzi, A. *et al.* Human mobility in response to covid-19 in france, italy and uk. *Scientific Reports* **11**, 1–10 (2021).

[16] Pullano, G., Valdano, E., Scarpa, N., Rubrichi, S. & Colizza, V. Evaluating the effect of demographic factors, socioeconomic factors, and risk aversion on mobility during the covid-19 epidemic in france under lockdown: a population-based study. *The Lancet Digital Health* **2**, e638–e649 (2020).

[17] Chinazzi, M. *et al.* The effect of travel restrictions on the spread of the 2019 novel coronavirus (covid-19) outbreak. *Science* **368**, 395–400 (2020).

[18] Kraemer, M. U. *et al.* The effect of human mobility and control measures on the covid-19 epidemic in china. *Science* **368**, 493–497 (2020).

[19] Rader, B. *et al.* Crowding and the shape of covid-19 epidemics. *Nature medicine* **26**, 1829–1834 (2020).

[20] Pepe, E. *et al.* Covid-19 outbreak response, a dataset to assess mobility changes in italy following national lockdown. *Scientific data* **7**, 1–7 (2020).

[21] Oidtman, R. J. *et al.* Trade-offs between individual and ensemble forecasts of an emerging infectious disease. *Nature communications* **12**, 5379–11 (2021).

[22] Lemey, P. *et al.* Untangling introductions and persistence in COVID-19 resurgence in Europe. *Nature* **595**, 713–717 (2021).

[23] Bassolas, A. *et al.* Hierarchical organization of urban mobility and its connection with city livability. *Nature communications* **10**, 1–10 (2019).

[24] Aguilar, J. *et al.* Impact of urban structure on infectious disease spreading. *Scientific reports* **12**, 3816 (2022).

[25] Hazarie, S., Soriano-Paños, D., Arenas, A., Gómez-Gardeñes, J. & Ghoshal, G. Interplay between population density and mobility in determining the spread of epidemics in cities. *Communications Physics* **4**, 1–10 (2021).

[26] Chang, S. *et al.* Mobility network models of covid-19 explain inequities and inform reopening. *Nature* **589**, 82–87 (2021).

[27] Kang, Y. *et al.* Multiscale dynamic human mobility flow dataset in the us during the covid-19 epidemic. *Scientific data* **7**, 1–13 (2020).

[28] https://www.istat.it/it/archivio/157423 (2011). [Accessed Feb-2021].

[29]https://www.census.gov/data/tables/2015/demo/metro-micro/commuting-flows-2015.html (2015). [Accessed Feb-2021].

[30]https://www.cuebiq.com/about/data-for-good (2020). [Accessed Feb-2021].

[31]https://dataforgood.facebook.com/dfg/tools (2020). [Accessed Feb-2021].